Hindawi Publishing Corporation
Laser Chemistry
Volume 2008, Article ID 656490, 6 pages
doi:10.1155/2008/656490

Research Article

Physical and Spectroscopic Properties of Yb^{3+}-Doped Fluorophosphate Laser Glasses

Shujiang Liu[1] and Anxian Lu[2]

[1] *Glass and Ceramic Key Laboratory, Shandong Institute of Light Industry, Jinan 250353, China*
[2] *School of Materials Science and Engineering, Central South University, Changsha 410083, China*

Correspondence should be addressed to Shujiang Liu, lsj_24@126.com

Received 24 April 2008; Accepted 4 August 2008

Recommended by Saulius Juodkazis

The physical properties including refractive index, Abbe number, nonlinear refractive index, microhardness and thermal expansion coefficient, and spectroscopic properties of Yb^{3+}-doped fluorophosphate laser glasses were investigated. The results show that due to the addition of fluoride, mechanical and thermal properties are promoted, emission cross-section σ_{emi} is also greatly enhanced. The largest gain coefficient $\sigma_{emi} \cdot \tau_m$ ($0.824\,pm^2 \cdot ms$) can be obtained with the minimum pump intensity I_{min} ($1.112\,kw/cm^2$). This kind of Yb^{3+}-doped fluorophosphate glass is an excellent candidate material for Yb^{3+}-doped host for high-power generation.

1. Introduction

With the rapid development of laser diode (LD) recently, Yb^{3+} doped laser materials as the gain medium in high-energy solid-state laser systems have obtained much attention [1–3]. There are only two manifolds in the Yb^{3+} energy level scheme, namely, the $^2F_{7/2}$ ground state and the $^2F_{5/2}$ excited state, and the absorption band is located at about 970 nm, with a large cross-section, which enables efficient pumping by high-power III–V diode lasers that are commercially available. The Yb^{3+} ions are also of interest not only as high-power lasers for nuclear fusion but also as energy transfer sensitizers for infrared lasers and up conversion lasers [4, 5]. The main obstacle is mechanical and thermal problems in the development of high-average powder solid-laser materials because more than half of pumping energy precipitate in gain medium, though effective semiconductor diode is used as pumping source, which results in various problems such as thermal load, mechanical stress. Therefore, in addition to high optical and spectroscopic properties, excellent thermal and mechanical properties are necessary, to improve the repetition rate of the laser glass.

For a long term, Yb^{3+} doped phosphate glasses have been regarded as ideal host matrix for high-power laser due to larger absorption and emission cross-section, less nonlinear refractive index [6–8]. However, the line-like network of phosphate glass results in higher thermal expansion coefficient (TEC), inferior physical properties such as mechanical and chemical durability [9, 10]. Furthermore, the hygroscopic tendency of phosphor lowers the fluorescence lifetime of Yb^{3+} ions. Some early researches [11, 12] have shown that formation of P–O–B(4) bonds in borophosphate glass could greatly improve physical properties along with broad emission bandwidth. However, the photo energy of B–O bond ($\sim 1400\,cm^{-1}$) is larger, so that the fluorescence lifetime of borate glass is less as compared to other glass. In order to improve the water resistance of phosphate glass, fluorophosphate glass is available because fluorophosphate glass has *m* advantages such as long fluorescene life time, low nonlinear refractive index [13, 14].

To obtain excellent physical and spectroscopic properties of Yb^{3+}-doped laser glass, we investigated the relationship between composition and mechanical, thermal and spectroscopic properties of fluorophosphate glasses.

2. Experimental

Two series of fluorophosphate glasses were chosen, and the glass compositions (mol%) listed in Table 1 were prepared by melting 100 g batches using analytical grade $(NH_4)_2HPO_4$,

Table 1: Chemical composition of Yb^{3+}-doped fluorophosphate glasses.

	A0	A1	A2	A3	A4	B1	B2	B3	B4
P_2O_5	63	63	63	63	63	44	44	44	44
Al_2O_3	7	7	7	7	7	7	7	7	7
Nb_2O_5	1	1	1	1	1	4	4	4	4
Li_2O	10	7.5	5	2.5	—	—	—	—	—
BaO	18	13.5	9	4.5	—	—	—	—	—
LiF	—	2.5	5	7.5	10	10	10	10	—
NaF	—	—	—	—	—	10	10	—	10
MgF_2	—	—	—	—	—	24	—	20	20
CaF_2	—	4.5	9	13.5	18	—	24	14	14
Yb_2O_3	1	1	1	1	1	1	1	1	1

Table 2: Physical properties of Yb^{3+}-doped fluorophosphate glasses.

	A0	A1	A2	A3	A4	B1	B2	B3	B4
Refractive index n_D	1.556	1.551	1.548	1.543	1.540	1.509	1.510	1.510	1.510
Abbe number ν	62.23	66.86	67.90	67.32	64.32	63.07	62.72	64.20	63.94
Nonlinear refractive index $n_2(\times 10^{-13}$ esu)	1.36	1.20	1.16	1.15	1.23	1.15	1.16	1.12	1.13
Microhardness (GPa)	3.68	3.75	3.89	3.95	4.10	4.40	4.16	4.20	4.11
Thermal expansion coefficient $\alpha(\times 10^{-7}/\mathrm{K})$	105.92	91.41	82.61	78.86	75.24	71.98	89.18	63.71	88.14

Al_2O_3, carbonate, Fluoride, Nb_2O_5, and Yb_2O_3 with a purity of above 99.99%. When each batch was slowly heated from room temperature up to 1000°C in a Al_2O_3 crucible, the crucible was covered to minimize the volatilization of phosphor, then the batch was melted at 1300~1320°C depending on the glass composition. Melts were quenched in stainless steel moulds and properly annealed. The final compositions of the glasses were checked by chemical analysis and found to be within ±1%.

The refractive index (n_D, n_F, and n_C) was measured on an Abbe refractometer (WZS-S) at room temperature at the wavelength of 589.3, 486.1, and 656.3 nm, respectively.

The microhardness of the investigated samples was measured using Vickers's microhardness indentor (MET-4). The eyepiece on the microscope of the apparatus allows measurements with an estimated accuracy of $\pm 0.5\,\mu$m for the indentation diagonal. Grinding and well polishing were necessary to obtain polished and flat parallel surfaces glass samples before indentation testing. At least five indentation readings were made and measured for each sample. Testing was conducted with a load of 30 g and loading time 15 seconds. The measurements were carried out under normal atmospheric condition.

Thermal expansion coefficient of the investigated glass was carried out on 2.0 cm long rods using AS-100 automatic recording multiplier dilatometer with heating rate of 5°C/min. The uncertainty of linear thermal expansion from room temperature to 300°C is $\pm 5 \times 10^{-7}$/°C.

The samples for measurement of spectroscopic properties were cut to a size of 20 mm × 20 mm × 2 mm with two larger sides polished. Absorption spectra were recorded with Perkin-Elmer (Lambda 900) UV/VIS/NIR spectrophotometer, at room temperature, in the range of 870–1150 nm. Emission spectra were measured with Triax 550 spectrophotometer through exciting the samples with a diode laser operating around 940 nm. The emission from the sample was focused to a monochrometer and detected by the Ge detector. The signal was intensified with a lock in amplifier and processed by a computer. Fluorescence lifetimes were measured by exciting the samples with a Xenon lamp and detected by an S-1 photomultiplier tube. The fluorescence decay curves were recorded and averaged with a computer-controlled transient digitizer.

3. Results

3.1. Physical Properties

Table 2 summarizes the data of measured refractive index, Abbe number, nonlinear refractive index, microhardness, and thermal expansion coefficient for fluorophosphate glass samples.

The knowledge of low nonlinear refractive index n_2 is required for laser applications to prevent spatial intensity fluctuations in the wavefront and self-focusing which lead to damage of optical components. n_2 can be calculated using the formula [15]:

$$n_2 = \frac{\left[68(n_D - 1)\left(n_D^2 + 2\right)^2\right] \times 10^{-13}}{\nu\left[1.517 + \left(n_D^2 + 2\right)(n_D + 1)\nu/6n_D\right]^{1/2}}\,\text{esu}, \quad (1)$$

where ν is Abbe number, $\nu = (n_D - 1)/(n_F - n_C)$. n_D is refractive index. It is clear that n_D constantly decreases in series A with increasing content of LiF and CaF_2 at the expense of Li_2O and BaO. It could mainly correlate with the difference of the polarizability of F^- and O^{2-}, furthermore,

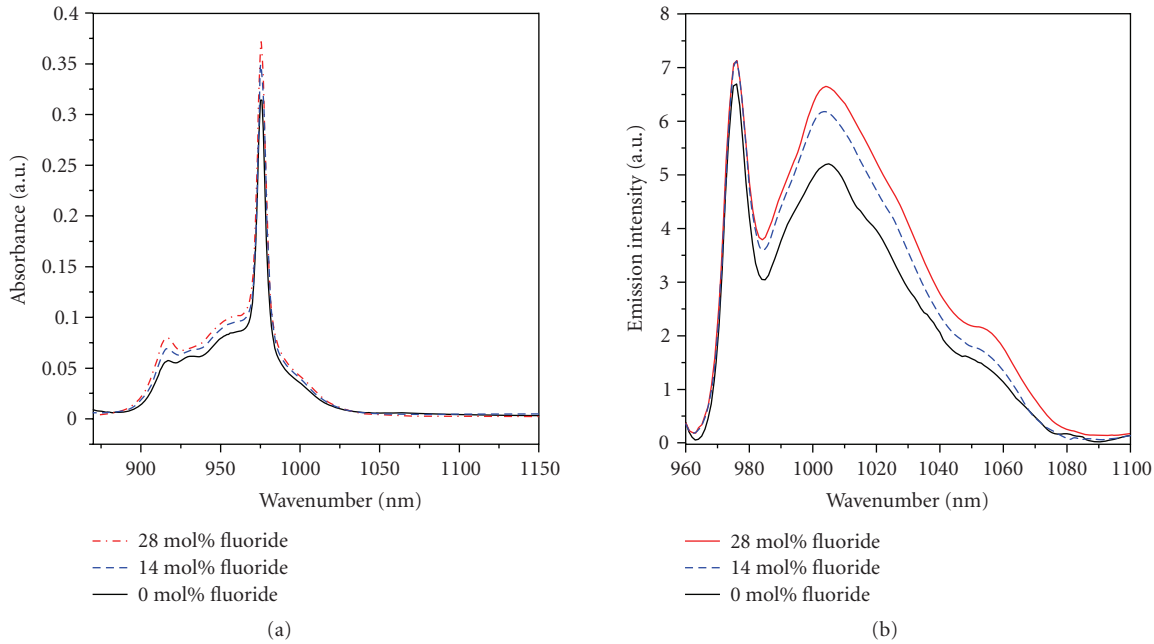

Figure 1: Absorption and emission spectra of Yb^{3+} in A0, A2, and A4 glasses.

introduction of Ca^{2+} with higher polarizing power than Ba^{2+} promotes this refractive index behavior. n_2 is minimized at A3. In the samples of series B, n_2 is only related to ν, since the values of n_D are nearly same, as shown in Table 2. Furthermore, n_2 appear inverse to ν according to (1), such B3 glass has the minimum n_2 due to its largest ν.

As shown in Table 1, with increasing fluoride content in the samples of series A, the microhardness increases gradually along with a decrease of thermal expansion coefficient. In series B, B1, and B3 glasses exhibit high microhardness and low-thermal expansion coefficient when compared to B2 and B4 on the same condition.

3.2. Spectroscopic Properties

The spectroscopic properties of Yb^{3+} ions in glasses are determined by transition between the four subenergy levels of $^2F_{7/2}$ and three subenergy levels of $^2F_{5/2}$, and the emission cross-section is associated with integral absorption cross-section $\sum_{abs}$ which can be obtained by (2) [16]:

$$\sum_{abs} = \int \sigma_{abs}(\lambda)d\lambda, \tag{2}$$

$$\sigma_{abs}(\lambda) = \left(\frac{2.303\log(I_0/I)}{Nl}\right), \tag{3}$$

where σ_{abs} is absorption cross-section, N is the Yb^{3+} ion concentration (ions/cm^3), and l is the thickness of the sample, $\log(I_0/I)$ is absorbance. The reciprocity method was used to calculate the emission cross-section of Yb^{3+} ions [17]:

$$\sigma_{emi}(\lambda) = \sigma_{abs}(\lambda)\frac{z_l}{z_\mu}\exp\left(\frac{E_{zl} - hc\lambda^{-1}}{kT}\right), \tag{4}$$

where Z_l/Z_u is the partition function; T is the absolute temperature; E_{zl} is the zero line energy, which is defined as the energy separation between the lowest components of the upper ($^2F_{5/2}$) and lower states ($^2F_{5/2}$); k, h, and c are Boltzman's constant, the Plank constant, and the velocity of light, respectively.

Spontaneous emission probability A_{rad} is calculated as follows [18]:

$$A_{rad} = \frac{1}{\tau_{rad}} = \frac{8\pi cn^2}{\lambda_p^4}\frac{2J'+1}{2J+1}\sum_{abs}, \tag{5}$$

where λ_p is the peak wavelength of absorption band, n is the refractive index at the peak wavelength, which is obtained from Cauchy's equation $n(\lambda) = A + B/\lambda^2$ according to the measured n_D, n_C, or n_F. J and J' are the total momentums for the upper and lower levels.

Figure 1 shows the absorption and emission spectra of the samples of series A. The line shape of absorption spectra is similar except intensity in all samples, the main absorption peak is around 975 nm (as shown in Figure 1(a)), which corresponds to the energy transition of the lowest subenergy level of $^2F_{5/2}$ and $^2F_{7/2}$. The absorption spectra is characterized by broader line widths due to out-of-order glass structure in which Yb^{3+} ions are localized in different coordination site and some portion of stark splitting energy overlap. As seen in Figure 1(b), the main emission peak of all samples is around 975 nm, and subemission peak is around 1006 nm which is mostly concerned. Other spectroscopic properties have been shown in Table 3.

In the Table 3, emission cross-section σ_{emi} and fluorescence lifetime τ_m gradually increase as the fluoride content increases from 0 to 28 mol% in series A glasses. Series B glasses shows larger integral absorption cross-section $\sum_{abs}$

Table 3: Spectroscopic properties of Yb^{3+}-doped fluorophosphate glasses.

	A0	A1	A2	A3	A4	B1	B2	B3	B4
Concentration (10^{20} ions/cm^3)	2.753	2.745	2.740	2.746	2.744	3.127	3.120	3.075	3.027
Σ_{abs}(10^4 pm^3)	3.93	3.86	3.54	3.65	3.73	4.76	4.84	5.49	5.51
σ_{emi}(pm^2)	0.598	0.601	0.608	0.649	0.653	0.915	0.947	1.065	1.032
A_{rad}(s^{-1})	982	1018	921	951	968	1188	1208	1371	1376
τ_m(ms)	0.84	0.87	0.98	1.03	1.08	0.89	0.87	0.73	0.75

and emission cross-section σ_{emi}, but less fluorescence lifetime τ_m compared to series A glasses.

4. Discussion

4.1. Effect of Fluoride on Mechanical and Thermal Properties

Excellent mechanical and thermal properties are indispensable to the laser driver for inertial confinement fusion (ICF), especially low-thermal expansion coefficient can reduce the thermal load of laser glasses, enhancing thermal shock toughness. As seen in Table 2, the microhardness increases and thermal expansion coefficient decreases when fluoride content gradually increases, moreover, the mechanical and thermal properties of series B glasses with higher fluoride content are superior to those of series A glasses. This anomalous behavior should be due to the structural change caused by the fluorides. It is clear from the glass composition as shown in Table 1 that the A0 glass without fluoride content mainly consists of metaphosphate (ΣMO: P_2O_5 = 1) group. Addition of fluorides leads to rupturing of long metaphosphate chains, $(PO_3^-)_n$ and the formation of short structural fragments of $P_2(O,F)_7$ and $P(O,F)_4$. However, these smaller fragments are linked up to a greater extent by the $Al(O,F)_6$ polyhedra [19], which leads to strengthening of the glass network. In particular, Nb^{5+} with higher field strength also promotes the linkage of smaller fragments in series B glasses. In addition, the fact that B1 and B3 glasses display better mechanical and thermal properties is also explained by the high cation field strength for Mg^{2+} and Li^+ ions.

4.2. Effect of Fluoride on Spectroscopic Properties

The emission cross-section σ_{emi} has an important effect on laser properties of Yb^{3+} ions because a larger σ_{emi} indicates higher laser gain [20]. From (4), it can be seen that the value of emission cross-section is only determined by the absorption cross-section, which removes the errors of reabsorption in the experiment of fluorescence spectrum. As seen in Table 3, the σ_{emi} increases with increase in fluoride content, and the increase of σ_{emi} depends on the change of structure of fluorophosphate glasses. Addition of fluoride leads to the reduction of P–O–P linkages due to a gradual transformation of $(PO_3^-)_n$ to $P_2(O,F)_7$ and $P(O,F)_4$, which decreases the connectivity of the glass network. This behavior is strengthened by the concentration of F^- ions. Moreover, the surrounding coordination Yb^{3+} ions are also changed due to present mixed anions, fluorine, and oxygen. In particular, the series B glasses with higher Nb_2O_5 and fluoride content contain different types of structural units such as $P_2(O,F)_7$, $P(O,F)_4$, $Al(O,F)_6$, and $Nb(O,F)_6$ in the framework of fluorophosphate glass, which increases asymmetry of the Yb^{3+} site environments and results in larger absorption and emission cross-section as shown in Table 3.

Generally, the decay rate for an excited state population, $\Gamma_m = 1/\tau_m$, is comprised of three processes: the radiative decay rate (Γ_r), the nonradiative decay rate (Γ_{nr}), and the additional nonradiative loss decay rate (Γ_q). The total decay rate is thus [21]:

$$\Gamma_m = \Gamma_r + \Gamma_{nr} + \Gamma_q = \frac{1}{\tau_r} + \frac{1}{\tau_{nr}} + \frac{1}{\tau_q}, \quad (6)$$

where τ_r, τ_{nr}, and τ_q are radiative decay, nonradiative decay, and additional nonradiative decay lifetime correspondingly. The radiative decay rate (Γ_r) is influenced by variations of the local crystal field symmetry at the rare-earth site. These variations are determined by the host matrix into which the ions are placed. Thus, τ_r depends on the ingredients around the Yb^{3+} ions and structure of host matrix. Since $Yb^{3+}(^2F_{5/2} \rightarrow {}^2F_{7/2})$ possesses the simple electronic energy level structure and nonradiative decay does not exist, the second process (Γ_{nr}) is negligible (i.e., $\Gamma_{nr} = 0$). The third process, Γ_q, represents an additional nonradiative loss mechanism which involves impurity or OH^- group [22]. For our glass samples starting with high purity materials, the effect of impurities can be little, so τ_q is dependent mostly on OH^- groups. Based on that, the total lifetime τ_m is influenced mostly by radiative decay and additional nonradiative loss by OH^- groups. OH^- groups decrease, Γ_q also decreases, then τ_q and τ_m increase correspondingly. As shown in Table 3, the τ_m increase with increase in fluoride content in series A glasses. This can be explained as follows: the hydroxyl and fluorine ions are isoelectronic with a similar ionic size, so that hydroxyl ions can be easily replaced by fluorine during melting, which decreases the traps of OH^- and prolongs the measured fluorescence lifetime. Whereas series B glasses exhibit shorter τ_m compared to series A glasses, this could be related to the difference of local environment around the Yb^{3+} ions in two host matrixes.

Table 4: Lasering properties of Yb^{3+}-doped fluorophosphate glasses.

	A0	A1	A2	A3	A4	B1	B2	B3	B4
$\sigma_{emi}\cdot\tau_m$(pm^2·millisecond)	0.502	0.523	0.596	0.668	0.705	0.814	0.824	0.777	0.774
I_{min}(kw/cm^2)	1.761	1.68	1.516	1.615	1.27	1.073	1.112	1.176	1.172

4.3. Effect of Fluoride on Laser Parameters

The minimum pump intensity I_{min} is a measure for the ease of pumping the laser material to get laser action. It is a very important parameter to evaluate the potential laser property. The lower the minimum pump intensity, the higher the pump efficiency, then the better laser property. I_{min} describes the minimum absorbed pump intensity that is required for transparency to be achieved at the extraction wavelength. I_{min} is calculated by the following equation [23]:

$$I_{min} = \beta_{min}\cdot I_{sat}, \tag{7}$$

where

$$\beta_{min} = \frac{\sigma_{abs}(\lambda_{laser})}{\sigma_{abs}(\lambda_{laser}) + \sigma_{emi}(\lambda_{laser})} = \left\{1 + \frac{Z_l}{Z_u}\exp\left(\frac{E_{zl} - hc\lambda_{laser}^{-1}}{kT}\right)\right\}, \tag{8}$$

$$I_{sat} = \frac{hc}{\lambda_{pump}\sigma_{abs}(\lambda_{pump})\tau_m},$$

where β_{min} is defined as the minimum fraction of Yb^{3+} ions that should be excited to balance the gain exactly with the ground state absorption at the laser wavelength. I_{sat} is the pumping saturation intensity that characterizes the pumping dynamics. Minimum values of β_{min}, I_{sat}, and I_{min} are apparently preferred in terms of laser properties. I_{min} is mainly determined by σ_{emi} and τ_m according to (7). The figure of merit of the Yb^{3+}-doped laser materials is given by the I_{min} and σ_{emi}, and it turns out to be given by the emission cross-section σ_{emi} and fluorescence lifetime τ_m. Therefore, the combination of higher σ_{emi}, longer lifetime τ_m, and lower minimum pump intensity I_{min} give a better Yb^{3+}-doped laser material. The parameters such as laser gain coefficient $\sigma_{emi}\cdot\tau_m$ and minimum pump intensity I_{min} are given in Table 4.

The $\sigma_{emi}\cdot\tau_m$ increases with increasing fluoride content in series A glasses, since addition of fluorine promotes emission cross-section σ_{emi} and fluorescence lifetime τ_m. In spite of shorter τ_m, series B glasses exhibit higher values of $\sigma_{emi}\cdot\tau_m$ and I_{min} due to higher σ_{emi} and the I_{min} of series B glasses is superior to the known QX/Yb glass [24]. Therefore, we believe that the fluorophosphate glasses are promising laser glasses for high-peak power and high-average power.

5. Conclusion

Yb^{3+}-doped fluorophosphate laser glasses have successfully been developed. A systematic investigation of physical properties including refractive index, Abbe number, nonlinear refractive index, microhardness, and thermal expansion coefficient has been performed as a function of fluoride content. With the increase of fluoride content, the microhardness increases gradually along with the decrease of thermal expansion coefficient. The structure around Yb^{3+} is simultaneously changed which greatly influences the spectroscopic properties and laser parameters. The best laser performance is found in $44P_2O_5$-$7Al_2O_3$-$4Nb_2O_5$-10LiF-$20MgF_2$-$14CaF_2$-$1Yb_2O_3$ glass system with the gain coefficient $\sigma_{emi}\cdot\tau_m$(0.824 pm^2·ms) and minimum pump intensity I_{min}(1.112 kw/cm^2). The favorable combination of outstanding physical, spectroscopic properties and laser parameters indicates that current Yb^{3+}-doped fluorophosphate glass is an excellent candidate material for Yb^{3+}-doped host for high-power generation.

Acknowledgment

This work is financially supported by the Chinese National Defense New Materials Project (MKPT-05-240).

References

[1] S.-X. Dai, L.-L. Hu, Z.-H. Jiang, G.-S. Huang, W. Chen, and P.-Z. Deng, "Study of ytterbium-doped phosphate and borate laser glasses," *Chinese Journal of Lasers*, vol. 29, no. 1, pp. 82–86, 2002 (Chinese).

[2] G. Karlsson, V. Pasiskevicius, A. Fragemann, J. Hellstom, and F. Laurell, "Generation of 100 kW-level pulses at 1.53 μm in the diode-pumped Er-Yb:glass laser-PPKTP optical parametric amplifier system," in *International Conference on Lasers, Applications, and Technologies 2002: Advanced Lasers and Systems*, vol. 5137 of *Proceedings of SPIE*, pp. 37–42, Moscow, Russia, June 2002.

[3] S. Blaize, L. Bastard, C. Cassagnètes, and J. E. Broquin, "Multiwavelengths DFB waveguide laser arrays in Yb-Er codoped phosphate glass substrate," *IEEE Photonics Technology Letters*, vol. 15, no. 4, pp. 516–518, 2003.

[4] L. Zhang and H. Hu, "Evaluation of spectroscopic properties of Yb^{3+} in tetraphosphate glass," *Journal of Non-Crystalline Solids*, vol. 292, no. 1–3, pp. 108–114, 2001.

[5] B. Peng and T. Izumitani, "Next generation laser glass for nuclear fusion," *The Review of Laser Engineering*, vol. 21, no. 12, pp. 1234–1244, 1993.

[6] J. H. Campbell, "Modeling platinum-inclusion dissolution in phosphate laser glasses," *Glass Science and Technology*, vol. 68, no. 3, pp. 96–101, 1995.

[7] C. Jiang, H. Liu, Q. Zeng, X. Tang, and F. Gan, "Yb: phosphate laser glass with high emission cross-section," *Journal of Physics and Chemistry of Solids*, vol. 61, no. 8, pp. 1217–1223, 2000.

[8] P. R. Ehrmann and J. H. Campbell, "Nonradiative energy losses and radiation trapping in neodymium-doped phosphate laser glasses," *Journal of the American Ceramic Society*, vol. 85, no. 5, pp. 1061–1069, 2002.

[9] S. Toyoda, S. Fujino, and K. Morinaga, "Density, viscosity and surface tension of 50RO-50P_2O_5 (R: Mg, Ca, Sr, Ba, and Zn) glass melts," *Journal of Non-Crystalline Solids*, vol. 321, no. 3, pp. 169–174, 2003.

[10] P. Y. Shih, S. W. Yung, and T. S. Chin, "FTIR and XPS studies of P_2O_5-Na_2O-CuO glasses," *Journal of Non-Crystalline Solids*, vol. 244, no. 2-3, pp. 211–222, 1999.

[11] P. A. Bingham, R. J. Hand, and S. D. Forder, "Doping of iron phosphate glasses with Al_2O_3, SiO_2 or B_2O_3 for improved thermal stability," *Materials Research Bulletin*, vol. 41, no. 9, pp. 1622–1630, 2006.

[12] H. Takebe, T. Harada, and M. Kuwabara, "Effect of B_2O_3 addition on the thermal properties and density of barium phosphate glasses," *Journal of Non-Crystalline Solids*, vol. 352, no. 6-7, pp. 709–713, 2006.

[13] L. Zhang, H. Sun, H. Wu, J. Wang, L. Hu, and J. Zhang, "Effects of PbF_2 on the spectroscopic, lasing and structural properties of Yb^{3+}-doped fluorophosphate glass," *Solid State Communications*, vol. 135, no. 1-2, pp. 150–154, 2005.

[14] J. H. Choi, A. Margaryan, A. Margaryan, and F. G. Shi, "Optical transition properties of Yb^{3+} in new fluorophosphate glasses with high gain coefficient," *Journal of Alloys and Compounds*, vol. 396, no. 1-2, pp. 79–85, 2005.

[15] J. H. Campbell and T. I. Suratwala, "Nd-doped phosphate glasses for high-energy/high-peak-power lasers," *Journal of Non-Crystalline Solids*, vol. 263-264, pp. 318–341, 2000.

[16] H. Takebe, T. Murata, and K. Morinaga, "Compositional dependence of absorption and fluorescence of Yb^{3+} in oxide glasses," *Journal of the American Ceramic Society*, vol. 79, no. 3, pp. 681–687, 1996.

[17] L. D. DeLoach, S. A. Payne, L. L. Chase, L. K. Smith, W. L. Kway, and W. F. Krupke, "Evaluation of absorption and emission properties of Yb^{3+} doped crystals for laser applications," *IEEE Journal of Quantum Electronics*, vol. 29, no. 4, pp. 1179–1191, 1993.

[18] D. C. Yeh, W. A. Sibley, M. Suscavage, and M. G. Drexhage, "Radiation effects and optical transitions in Yb^{3+} doped barium-thorium fluoride glass," *Journal of Non-Crystalline Solids*, vol. 88, no. 1, pp. 66–82, 1986.

[19] B. Karmakar, P. Kundu, and R. N. Dwivedi, "IR spectra and their application for evaluating physical properties of fluorophosphate glasses," *Journal of Non-Crystalline Solids*, vol. 289, no. 1–3, pp. 155–162, 2001.

[20] X. Zou and H. Toratani, "Evaluation of spectroscopic properties of Yb^{3+} -doped glasses," *Physical Review B*, vol. 52, no. 22, pp. 15889–15897, 1995.

[21] T. Miyakawa and D. L. Dexter, "Phonon sidebands, multiphonon relaxation of excited states, and phonon-assisted energy transfer between ions in solids," *Physical Review B*, vol. 1, no. 7, pp. 2961–2969, 1970.

[22] L. Zhang, H. Hu, C. Qi, and F. Lin, "Spectroscopic properties and energy transfer in Yb^{3+}/Er^{3+}-doped phosphate glasses," *Optical Materials*, vol. 17, no. 3, pp. 371–377, 2001.

[23] L. D. DeLoach, S. A. Payne, L. K. Smith, W. L. Kway, and W. F. Krupke, "Laser and spectroscopic properties of $Sr_5(PO_4)_3F$:Yb," *Journal of the Optical Society of America B*, vol. 11, no. 2, pp. 269–276, 1994.

[24] U. Griebner, R. L. Koch, H. Schonnagel, et al., "Laser performance of a new ytterbium doped phosphate laser glass," in *Proceedings of the OSA Topical Meeting on Advanced Solid-State Lasers (ASSL '96)*, S. A. Payne and C. R. Pollock, Eds., vol. 1, pp. 26–29, OSA, San Francisco, Calif, USA, January-February 1996.